Am. J. Hum. Genet. 69:722–737, 2001

CNGA3 Mutations in Hereditary Cone Photoreceptor Disorders

Bernd Wissinger,[1,3] Daphne Gamer,[1,3] Herbert Jägle,[2,3] Roberto Giorda,[4] Tim Marx,[1,3] Simone Mayer,[1,3] Sabine Tippmann,[1,3] Martina Broghammer,[1,3] Bernhard Jurklies,[5] Thomas Rosenberg,[6] Samuel G. Jacobson,[7] E. Cumhur Sener,[8] Sinan Tatlipinar,[8] Carel B. Hoyng,[9] Claudio Castellan,[11] Pierre Bitoun,[12] Sten Andreasson,[13] Günter Rudolph,[14] Ulrich Kellner,[15] Birgit Lorenz,[16] Gerhard Wolff,[17] Christine Verellen-Dumoulin,[18] Marianne Schwartz,[6] Frans P. M. Cremers,[10] Eckart Apfelstedt-Sylla,[3] Eberhart Zrenner,[3] Roberto Salati,[4] Lindsay T. Sharpe,[2,3,19] and Susanne Kohl[1,3]

[1]Molekulargenetisches Labor, [2]Psychophysisches Labor, and [3]Universitäts-Augenklinik Tübingen, Abt. Pathophysiologie des Sehens und Neuroophthalmologie, Tübingen, Germany; [4]Laboratory of Molecular Biology and Department of Pediatric Ophthalmology, IRCCS Eugenio Medea, Bosisio Parini, Italy; [5]Universitäts-Augenklinik Essen, Essen, Germany; [6]National Eye Clinic, Copenhagen; [7]Scheie Eye Institute, Philadelphia; [8]Hacetteppe University, Ankara; Departments of [9]Ophthalmology and [10]Human Genetics, University Medical Center, Nijmegen, The Netherlands; [11]Genetische Beratungsstelle, Bozen, Italy; [12]University Hospital Jean Verdier Paris-Nord, Bondy, France; [13]University Eye Hospital Lund, Lund, Sweden; [14]Universitäts-Augenklinik München, München, Germany; [15]Augenklinik, Klinikum Benjamin Franklin, Free University, Berlin; [16]Abteilung für Kinderophthalmologie, Strabismologie und Ophthalmogenetik, Universitäts-Augenklinik Regensburg, Regensburg, Germany; [17]Institut für Humangenetik und Anthropologie, Universität Freiburg, Freiburg, Germany; [18]Centre de Génétique Humaine, Université Catholique de Louvain, Louvain, Belgium; and [19]Department of Psychology, University of Newcastle, Newcastle-upon-Tyne

We recently showed that mutations in the *CNGA3* gene encoding the α-subunit of the cone photoreceptor cGMP-gated channel cause autosomal recessive complete achromatopsia linked to chromosome 2q11. We now report the results of a first comprehensive screening for *CNGA3* mutations in a cohort of 258 additional independent families with hereditary cone photoreceptor disorders. *CNGA3* mutations were detected not only in patients with the complete form of achromatopsia but also in incomplete achromats with residual cone photoreceptor function and (rarely) in patients with evidence for severe progressive cone dystrophy. In total, mutations were identified in 53 independent families comprising 38 new *CNGA3* mutations, in addition to the 8 mutations reported elsewhere. Apparently, both mutant alleles were identified in 47 families, including 16 families with presumed homozygous mutations and 31 families with two heterozygous mutations. Single heterozygous mutations were identified in six additional families. The majority of all known *CNGA3* mutations (39/46) are amino acid substitutions compared with only four stop-codon mutations, two 1-bp insertions and one 3-bp in-frame deletion. The missense mutations mostly affect amino acids conserved among the members of the cyclic nucleotide gated (CNG) channel family and cluster at the cytoplasmic face of transmembrane domains (TM) S1 and S2, in TM S4, and in the cGMP-binding domain. Several mutations were identified recurrently (e.g., R277C, R283W, R436W, and F547L). These four mutations account for 41.8% of all detected mutant *CNGA3* alleles. Haplotype analysis suggests that the R436W and F547L mutant alleles have multiple origins, whereas we found evidence that the R283W alleles, which are particularly frequent among patients from Scandinavia and northern Italy, have a common origin.

Introduction

Human daylight and color vision relies on the presence and functional integrity of three types of retinal photoreceptors—the cones sensitive to short (blue), middle (green), and long (red) wavelengths—which are characterized by the expression of specific visual pigments (cone opsins). Color discrimination depends on the differential excitation of the cone pigments by light stimuli of specific wavelengths and the appropriate processing of the postreceptor signals. Functional loss or alterations in the spectral properties of one type of cone photoreceptors—as caused by mutations, deletions, or structural rearrangements of one of the opsin genes—may result in selective color-vision deficiencies, such as the common forms of X-linked red-green color blindness (protan and deutan defects) or the less frequent autosomal dominant inherited blue-yellow (tritan) deficiency (Nathans et al. 1986; Weitz et al. 1992; for a review, see Sharpe et al. 1999). More-general forms of color blindness involve

Received May 24, 2001; accepted for publication July 31, 2001; electronically published August 30, 2001.

Address for correspondence and reprints: Dr. Bernd Wissinger, Molekulargenetisches Labor, Universitäts-Augenklinik, Auf der Morgenstelle 15, D-72076 Tübingen, Germany. E-mail: wissinger@uni-tuebingen.de

0002-9297/2001/6904-0007$02.00

the degeneration, dysfunction, or absence of two or more types of cone photoreceptors, as in patients with achromatopsia or cone dystrophies.

Whereas patients with cone dystrophy may secondarily develop total color blindness following the progressive degeneration of cone photoreceptors, the term "achromatopsia" denotes a group of congenital and stationary retinal disorders with normal rod function but with absent or limited cone photoreceptor function associated with photophobia and nystagmus. Complete achromatopsia (also referred to as "rod monochromacy" or "total color blindness") is defined by the absence of measurable cone photoreceptor function. Patients are totally color blind, visual acuity is <0.2, there is severe photophobia under daylight conditions, and nystagmus is evident within the first month after birth. Complete achromatopsia is inherited as an autosomal recessive trait. Its prevalence has been estimated to be ≤1:30,000 (Francois 1961; Sharpe and Nordby 1990; Sharpe et al. 1999).

Residual cone function—either measured by ERG recordings and/or assessed on the basis of performance on color tests—essentially distinguishes incomplete from complete achromatopsia. The severity of symptoms (i.e., visual-acuity loss, photophobia) is generally less pronounced than with complete achromats. However, there is considerable variability in the clinical manifestation among incomplete achromats. In particular, color testing performance varies markedly—ranging from nearly normal performance, with specific axes of confusion, to negligible color-matching ability—and depends on the type of test used (Jäger 1953; Goodman et al. 1963; Neuhann et al. 1978; Jägle et al. 2001). Most cases of incomplete achromatopsia are sporadic or occur among siblings, consistent with an autosomal recessive mode of inheritance. The molecular basis of incomplete achromatopsia is largely unknown. One notable exception is blue cone monochromacy (BCM [MIM 303700]), a particular form of incomplete achromatopsia that is caused by mutations in a solitary red or red-green hybrid opsin gene, simultaneous mutations in both red and green opsin genes, or deletions within the adjacent locus control region (Nathans et al. 1993). Acceptance of blue filter glasses for improving contrast vision, color discrimination along the blue-yellow axis, and X-linked inheritance distinguish BCM from other forms of achromatopsia (Hansen 1979; Zrenner et al. 1988; Andreasson and Tornqvist 1991; Sharpe et al. 1999).

By means of linkage analysis, two loci for complete achromatopsia, *ACHM2* (MIM 216900) and *ACHM3* (MIM 262300), have been identified on chromosomes 2q11 and 8q21, respectively (Arbour et al. 1997; Wissinger et al. 1998; Milunsky et al. 1999; Winick et al. 1999). Subsequently, we showed that mutations in the *CNGA3* gene (MIM 600053) cause complete achromatopsia in families that show linkage to the *ACHM2* locus (Kohl et al. 1998), and, more recently, we and others were able to identify the *CNGB3* gene (MIM 605080) that is mutated in families segregating disease with the *ACHM3* locus (Kohl et al. 2000; Sundin et al. 2000). *CNGA3* and *CNGB3* encode the α- and putative β-subunits of the cone photoreceptor cGMP-gated channel (cone CNG channel), which represents a crucial component of the cone phototransduction cascade. Whereas high levels of cGMP in the photoreceptor outer segment keep the CNG channel open for cation influx in the dark, light stimulation results in a decrease of the cGMP level and, subsequently, in the closure of the CNG channel. This closure shuts off the steady inward current and thus generates a membrane hyperpolarization signal that decreases the glutamate release at the photoreceptor synapse (Müller and Kaupp 1998). When the importance of the CNG channel in phototransduction is considered, the phenotype of achromatopsia can be well explained as a result of mutations in the *CNGA3* or *CNGB3* gene. Furthermore, it implies that the same CNG channel is common to all three types of cone photoreceptors. Analysis of the homologous *CNGA3* knockout–mouse model shows complete absence of physiologically measurable cone function, a decrease in the number of cones in the retina, and morphological abnormalities of the remaining cones (Biel et al. 1999). These results accord with the four histological examinations that have been made of human purported achromat eyes, although the extent of loss in cone number and their regional distribution varied considerably, and at least one of the cases was more consistent with cone dystrophy (Larsen 1921; Harrison et al. 1960; Falls et al. 1965; Glickstein and Heath 1975; Sharpe and Norby 1990). Variability in histological presentation may reflect heterogeneity in the genetic etiology of achromatopsia and/or inclusion of cases with complete and incomplete achromatopsia.

In our initial article on *CNGA3* mutations, we described eight different missense mutations segregating in five families with complete achromatopsia (Kohl et al. 1998). Since then, we have completed a large-scale screening of the *CNGA3* gene, which now provides deeper insight into this causal relationship, as well as into a number of related issues: (i) the prevalence of *CNGA3* mutations in achromatopsia, (ii) the allelic heterogeneity of *CNGA3* mutations, (iii) the recurrence rate and origin of common *CNGA3* mutations, and (iv) the spectrum of cone photoreceptor disorders caused by *CNGA3* mutations. Although our original families with *CNGA3* mutations have been categorized with complete achromatopsia, we hypothesized that *CNGA3* alleles might exist that do not completely abolish cone function and thus may result in incomplete achromatopsia. Given that mutations in the homologous gene

in rod photoreceptors cause retinitis pigmentosa, a progressive form of retinal dystrophy (Dryja et al. 1995), and that degenerative processes have been noticed in some patients with BCM and incomplete achromatopsia (Goodman et al. 1963; Neuhann et al. 1978; Ayyagari et al. 1999), we also included patients diagnosed with progressive cone dystrophy in this study.

Subjects, Material, and Methods

Patients and Clinical Examination

Patients were examined in several clinical centers in Germany, The Netherlands, Denmark, Italy, Sweden, France, Turkey, and the United States. The largest numbers of patients were of apparent German (~37%), Dutch (~18%), Danish (~12%), and Italian (~12%) origins. Clinical diagnosis was based on disease history, routine ophthalmological examination, and specialized visual function testing, such as color vision tests, scotopic and photopic electroretinography (ERG), and dark-adapted psychophysics. In addition, a patients' questionnaire was used which addressed the family history, subjective views about major visual complaints, onset and course of the disease, a history or presence of additional nonretinal diseases (namely heart or kidney diseases or male infertility), impairments of other sensory systems (namely hearing, balance, taste, and smell) and the presence of sleep disorders or impairment of day-night rhythms.

The index patient sample comprises 215 independent patients (including those five described elsewhere by Kohl et al. [1998]) with a diagnosis of congenital achromatopsia, either complete or incomplete, and 48 independent patients with cone dystrophy. Criteria used in this study for diagnosis of the three different types of cone disorders were as follows:

Complete achromatopsia.—These patients have visual acuity <0.2, nystagmus or a history of nystagmus in childhood, severe photophobia, no measurable response to conventionally performed light-adapted (photopic) or 30-Hz flicker cone ERGs but normal rod function, complete inability to perform color-discrimination tasks, and a normal fundus.

Incomplete achromatopsia.—These patients have reduced visual acuity and may or may not have nystagmus or photophobia. Whereas the degree of cone dysfunction can vary considerably, rod function is not impaired. Patients have residual cone ERG responses and/or color-matching capabilities which distinguish such patients from those with complete achromatopsia. The fundus is normal.

Cone dystrophy.—These patients have the visual function findings of achromats, but there is evidence of progressive loss of vision (sometimes including the rods) and fundus abnormalities, such as macular degenerative changes or peripheral retinopathy. Venous blood was collected from the patients and available family members after informed consent was given, and total genomic DNA was extracted according to standard procedures.

Mutation Screening

Exons and flanking intron sequences of the *CNGA3* gene were amplified by PCR from total genomic DNA (Kohl et al. 1998) and were subjected to direct DNA sequencing or SSCP analysis. Initially, mutation screening was done by sequence analysis of both strands for all coding exons (exons 1–7) and flanking intron/untranslated sequences. In later stages of the project, we adopted a more practical screening protocol: (i) sequence analysis of exon 7, (ii) sequence or SSCP analysis of exons 5 and 6, and (iii) sequence analysis of all remaining exons, including exons 2b and 0 in those patients in whom only a single heterozygous mutation had been identified to that point.

For SSCP analysis, PCR products were separated on 10% polyacrylamide gels (with or without 10% glycerol) in 1 × TBE at 4°C or room temperature and were silver stained. For direct sequencing, PCR products were purified by Centricon-100 ultrafiltration (Amicon) or Qiaquick columns (Qiagen) and were subjected to DNA sequencing employing the Ampli*Taq* FS Dye Terminator or, in later stages, the BigDye Terminator Chemistry (PE Applied Biosystems). Sequences were separated on an ABI 373A or an ABI 377 DNA sequencer (PE Applied Biosystems), were analyzed manually and independently by two experimenters and were assembled with the SeqMan program (DNASTAR).

Cosegregation analysis and exclusion of the mutations in control subjects ($n = 100$) was done either by PCR/RFLP or SSCP analysis. Primer sequences and RFLP assay conditions are available from the authors upon request.

Polymorphisms and Haplotype Analysis

Genotyping of microsatellite markers *D2S2187, D2S2311,* and *CNGA3-STR* was performed by PCR amplification from genomic DNA through use of fluorescence-labeled primers, separation of the products on 5% polyacrylamide/8 M urea gels on an ABI 373 DNA sequencer (PE Applied Biosystems), and analysis with the Genescan software program, as described elsewhere (Wissinger et al. 1998). Intragenic SNP genotyping was done by PCR/RFLP analysis: 72T→C results in the loss of a *Bgl*II site; 102-16A→G results in the loss of an *Nsi*I site after amplification with mismatch-containing (MM) primer CNGA3-PMNsiI (5′-TTG AAA TCA ATT CTG CTT GAT GC-3′ [mismatch underlined]); 215+46T→G results in the gain of a *Bgl*I site after amplification with MM primer CNGA3-PMBglI (5′-TTA TTA TGG CCT

GGG GGC CAC TGT-3′); and 215+151T→C results in the gain of a *Cac*8I site after amplification with MM primer CNGA3-PMCac8I (5′-ACA TCT GAC CCA AGA GGA AAT TGC TC-3′). Disease haplotypes were reconstructed on the basis of the allele segregation within individual families. In addition, nondisease haplotypes were reconstructed to serve as controls for allele and haplotype frequencies among the study population. In some individuals with noninformative results for SNPs 215+46T→G or 215+151T→C, the phase could be resolved by double digests with *Bgl*I and *Cac*8I.

Haplotypes that could not be reconstructed unequivocally—either because of noninformative allele segregation of markers or because samples from critical family members were not available—were considered as conforming with the common haplotype for this mutation if one of the observed alleles matched the common allele.

RNA Isolation, RT-PCR, and RACE

Total RNA was isolated from human donor retinas and the human retinoblastoma cell line WERI-Rb1 by use of Trizol reagent (Life Technologies). Three-microgram aliquots of total RNA were reverse transcribed into single-stranded cDNA with AMV reverse transcriptase and oligo(dT) adaptor primers (RNA PCR Kit, Takara). cDNA aliquots were used to amplify overlapping segments of the 5′ portion of *CNGA3*. For 5′ RACE, ~20 ng of Marathon-Ready Human Retinal cDNA (Clontech) was subjected to nested PCR amplifications with adaptor primers and *CNGA3* cDNA primers. RT-PCR and RACE products were gel purified and were cloned with the TA Cloning System (Invitrogen). The isolated plasmid DNA was sequenced with standard pUC/M13 forward and reverse primers.

Isolation of PAC Clones

PAC clones were isolated by hybridization against a high-density filter of a human chromosome 2 library (Gingrich et al. 1996) or by PCR screening of pools of the RPCI1 library (Ioannou and de Jong 1996) provided by the U.K. Human Genome Mapping Project (HGMP) resource center. PAC DNA was isolated by standard alkaline lysis protocols, and the insert size was determined by PFGE separation of *Not*I-digested PAC DNA. STS content mapping was performed with 500 pg of PAC DNA and PCRs limited to 23–25 thermal cycles. PAC DNA was subcloned into the partially filled-in *Xho*I site of pBluescript SKII$^+$ vectors by limited digestion of PAC DNA with *Bsp*143I, partial fill-in of the 5′ protruding ends, and isolation of 8–15-kb fragments from preparative agarose gels.

Database Sequences and Amino Acid–Sequence Alignment

The GenBank sequences used to construct an alignment of CNG channels' protein sequences and to analyze the evolutionary conservation of corresponding amino acid positions (table 1) were: the CNG channel α-subunits of human cone photoreceptors (accession number AF065314), of mouse cone photoreceptors (AJ243933), of chicken cone photoreceptors (X89598), of human rod photoreceptors (S42457), and of bovine olfactory epithelium (X55010); the *Drosophila melanogaster* CNG channel (X89601); and the *Caenorhabditis elegans tax4* CNG channel (D89601). Sequences were aligned using the CLUSTAL algorithm implemented in the MEGALIGN program of the DNASTAR software package. Probability values for the equal distribution of mutations (i.e., evolutionarily conserved amino acid positions vs. nonconserved positions) were calculated using the χ^2 test.

Results

Genomic Structure and Additional Exons of the CNGA3 *Gene*

We recently reported the entire coding sequence of the human *CNGA3* gene and its genomic structure, composed of seven exons (Wissinger et al. 1997). Using RACE and RT-PCR, we were able to extend the *CNGA3* cDNA by an additional 168 bp of 5′ untranslated sequence. This sequence is encoded by an extra exon, designated "exon 0" and localized ~24 kb upstream of exon 1 (fig. 1). Exon 0 and the downstream intron sequence are enriched for -CG- dinucleotides, suggesting that the newly identified sequence is in close proximity to the actual transcription initiation site. In addition, we found a 38-bp-long sequence segment overlapping with the ultimate 5′ end of the human cDNA to be almost completely identical to the 5′ end of the orthologous bovine cDNA (fig. 1*b*). The evolutionary conservation of this sequence implies that it may bear some specific function—for example, in transcription regulation.

During our efforts to identify additional 5′ sequences, we recurrently observed a retinal splicing variant that includes an additional 165 bp of coding sequence between exons 2 and 3. This additional exon, designated "exon 2b," extends the low conserved aminoterminal part of the CNGA3 polypeptide by 55 amino acids (fig. 1*c*). No other known CNG channel contains sequences homologous to those encoded by exon 2b, and database searches provided no significant similarities with other proteins. Thus, the functional relevance of this sequence and the splice variant itself remain unclear.

On the basis of our sequence analysis of PAC clones isolated for the *CNGA3* gene and the database sequence

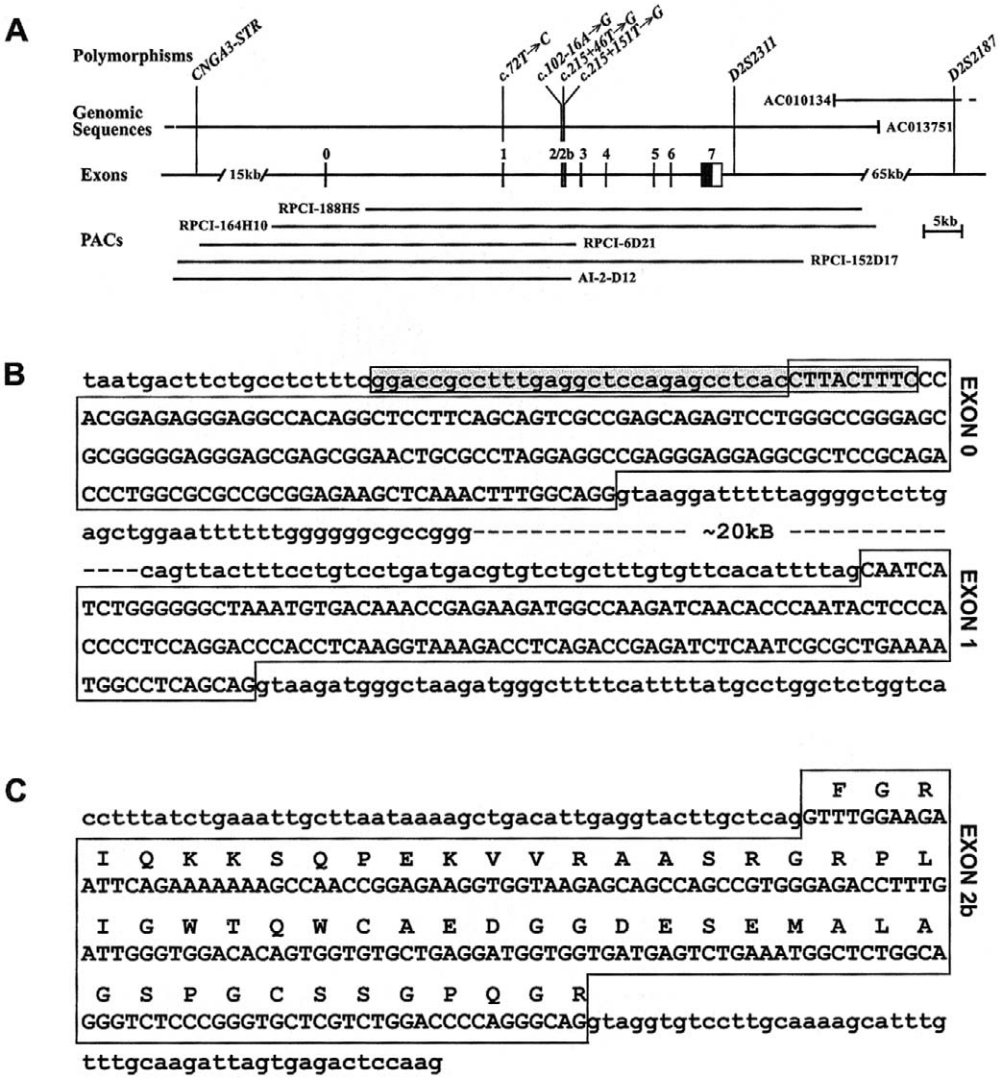

Figure 1 Genomic structure of the *CNGA3* gene and sequences of newly identified exons. *A*, Schematic genomic map of the *CNGA3* gene covered by two finished BAC sequences (AC013751 and AC010134) and additional PAC clones isolated from the RPCI1 library and a chromosome 2–specific LLNL library (AI-2-D12). The *CNGA3* gene is composed of nine exons, including the newly identified exons 0 and 2b. The locations of STR and SNP markers used for haplotype analysis are indicated at the top. *B*, Nucleotide sequence of exons 0 and 1 and flanking sequences. cDNA sequences are boxed and are shown in uppercase letters, whereas flanking 5′ genomic and intron sequences are given in lowercase letters. Note that the extent of exon 0 was deduced from the longest 5′ RACE clone. A 38-bp segment conserved between the human *CNGA3* gene and the 5′ UTR of the orthologous bovine cDNA is highlighted by a gray box. *C*, Nucleotide sequence of the alternatively spliced exon 2b and flanking intron sequences. The exon sequence is boxed and is shown in uppercase letters, with the deduced in-frame amino acid sequence shown above it as single-letter codes.

of BAC clone RP11-629A22 (GenBank accession number AC027241), the entire *CNGA3* gene covers ~53 kb of genomic sequence (fig. 1*a*). The markers *D2S2311* and *D2S2187* (located on the overlapping BAC clone RP11-127K18 [GenBank accession number AC010134]) were identified ~1.6 kb and ~90 kb downstream of the polyadenylation site, respectively, and thus represent the indexed genetic markers closest to the *CNGA3* gene (fig. 1*a*). Another CA-dinucleotide repeat was found ~27 kb upstream of the 5′-terminal exon 0 and was used to develop an additional polymorphic dinucleotide marker, *CNGA3-STR*, for segregation analysis and haplotype construction (see below).

Mutation Screening

Mutation screening was performed in a total sample of 258 independent index patients. *CNGA3* mutations were identified in 53 of those patients. Notably, mutations were not confined to the group of patients with

Table 1

***CNGA3* Mutations**

Alteration of Nucleotide Sequence[a]	Alteration Polypeptide[b,c]	No. of Chromosomes[d]	Evolutionary Conservation[e]						
			HC	MC	CC	HR	BO	DM	CE
Exon 2:									
148insG	G49fs	1							
Exon 5:									
485A→T	D162V	1	D	D	D	D	D	D	D
488C→T	P163L*	3	P	P	P	P	P	P	P
542A→G	Y181C	2	Y	Y	Y	Y	Y	Y	Y
544A→T	N182Y	1	N	N	N	N	N	N	N
556C→T	L186F	1	L	L	L	V	L	V	V
Exon 6:									
572G→A	C191Y	3	C	C	C	C	C	V	V
580G→A	E194K	1	E	E	E	E	D	E	D
667C→T	R223W	3	R	R	R	R	R	H	R
671C→G	T224R	1	T	T	T	T	T	E	M
Exon 7:									
778G→A	D260N	1	D	D	D	D	D	D	D
800G→A	G267D	1	G	G	G	G	G	P	I
829C→T	R277C	9	R	R	R	R	R	R	R
830G→A	R277H	2	R	R	R	R	R	R	R
847C→T	R283W*	19	R	R	R	R	R	R	R
848G→A	R283Q*	2	R	R	R	R	R	R	R
872C→G	T291R*	1	T	T	T	T	T	T	T
934-936delATC	I312del	3	I	I	I	I	I	V/L/I[f]	I
947G→A	W316X	1							
1021T→C	S341P	1	S	S	S	N	T	N	N
1106C→G	T369S	1	T	T	T	T	T	T	V
1114C→T	P372S	3	P	P	P	P	P	P	P
1139T→C	F380S	1	F	F	F	F	F	F	F
1217T→C	M406T	1	M	M	M	M	M	M	M
1228C→T	R410W*	3	R	R	R	R	R	R	R
1279C→T	R427C	3	R	R	R	R	R	R	R
1306C→T	R436W	6	R	R	R	R	K	R	R
1320G→A	W440X	1							
1350insG	V451fs	1							
1412A→G	N471S	1	N	N	N	N	N	Q	Q
1454A→T	D485V	1	D	D	D	D	D	D	D
1529G→C	C510S	2	C	C	C	C	C	C	C
1538G→A	G513E	1	G	G	G	G	G	G	G
1547G→A	G516E	1	G	G	G	G	G	G	G
1565T→C	I522T	1	I	I	I	I	I	V	V
1574G→A	G525D	1	G	G	G	G	G	G	G
1585G→A	V529M*	1	V	V	V	V	V	V	V
1609C→T	Q537X	1							
1641C→A	F547L*	12	F	F	F	F	F	F	F
1669G→A	G557R*	2	G	G	G	G	G	G	G
1688G→A	R563H	3	R	R	R	R	R	R	R
1694C→T	T565M	2	T	T	T	T	T	T	T
1706G→A	R569H	1	R	R	R	K	R	R	R
1718A→G	Y573C	1	Y	Y	Y	Y	Y	Y	Y
1777G→A	E593K	1	E	E	E	D	D	E	D
1963C→T	Q655X	1							

[a] Sequence position within the *CNGA3* cDNA, with 1 denoting the first nucleotide of the ATG start codon.

[b] fs = frameshift.

[c] Mutations reported by Kohl et al. (1998) are marked by asterisks (*).

[d] Number of observed mutant chromosomes.

[e] Corresponding amino acid residues in the sequences of the following CNG gated channels: HC = human cone; MC = murine cone; CC = chicken cone; HR = human rod; BO = bovine olfactory epithelium; DM = *Drosophila melanogaster;* and CE = *Caenorhabditis elegans-tax4* (see Subjects, Material, and Methods).

[f] Alternatively aligned amino acids.

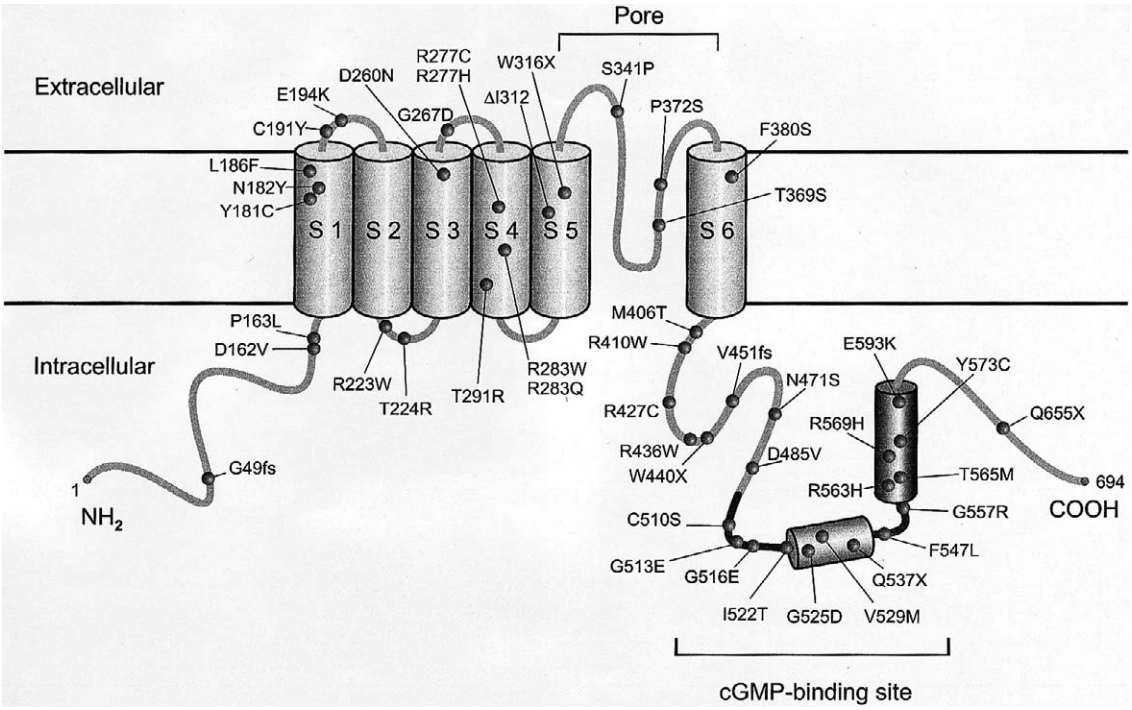

Figure 2 Location of the mutations with respect to the proposed topological model of the CNGA3 polypeptide including the six transmembrane helices (S1–S6), the ion pore, and the cGMP-binding domain (modified according to Zagotta and Siegelbaum [1996]).

complete achromatopsia but were also found in patients with incomplete forms of achromatopsia and even in a few patients diagnosed with cone dystrophy (see below).

Apparently homozygous mutations were found in 16 patients, and another 31 patients carried two heterozygous mutations. However, homozygosity could be mimicked by the presence of heterozygous deletions, and two heterozygous mutations might be present in *cis*. To exclude these possibilities, segregation analysis of the mutations was performed within the respective families. True homozygosity could be established in all cases in which both parents could be genotyped (12/16). Similarly, for the cases with two heterozygous mutations, we could experimentally verify their independent inheritance (allelism) in all cases in which samples from unaffected family members were available (23/31). Moreover, the segregation patterns of mutations within families were consistent with respect to the affection status and confirmed the presence of both mutant alleles in 16 other affected family members (not shown).

Only single heterozygous mutations were identified in an additional six index patients. In these patients, all exons of the *CNGA3* gene (including exons 0 and 2b) were sequenced, and large structural alterations of the *CNGA3* gene were ruled out by Southern blot hybridization in selected patients.

We identified a total of 38 new *CNGA3* mutations, in addition to the 8 mutations reported elsewhere (table 1; Kohl et al. 1998). In the combined sample of known *CNGA3* mutations, the vast majority (39/46) represent amino acid substitutions, compared with only 4 stop-codon mutations, 2 single-codon insertions, and 1 single-codon in-frame deletion. Among the single-base–substitution mutations (missense plus stop-codon mutations), there were 35 transitions and 8 transversions, and a preponderance of guanine and cytosine nucleotides (33/43) affected by mutations. We observed the typical increased incidence of mutations in -CG- dinucleotides (10/43). This accounts at least in part for the high frequency of substitutions at arginine codons (10 of 39 missense mutations; table 1).

The distribution of mutations in *CNGA3* is biased towards the central and terminal segments of the gene. Only a single mutation, 148insG (G49fs), was observed within the first six exons (exons 0, 1, 2, 2b, 3, and 4); all other mutations are located in the three terminal exons (exons 5, 6, and 7). With the exception of the early frameshift mutation, G49fs, and the terminal stop-codon mutation, Q655X, all remaining mutations are concentrated between amino acid positions 162 and 593, a region that accounts for less than two-thirds of the coding sequence (fig. 2). Thus the mutations are mainly confined to the functionally and structurally important central parts of the *CNGA3* polypeptide, including the

six transmembrane helices (S1–S6), the ion pore, and the cGMP-binding domain. An apparent clustering of mutations can be seen at the terminus of transmembrane helix S1 (amino acid positions 181–194), transmembrane helix S4 (amino acid positions 277–291) and parts of the cGMP-binding domain (amino acid positions 510–529 and 557–573). Excluding the frameshift and stop codon mutations, 40 amino acid positions in the *CNGA3* gene are affected by mutation. All these amino acids are at least conserved among cone CNG channel α-subunits, and 27 of them are even conserved among the various CNG channels in vertebrate photoreceptors and the olfactory epithelium, as well as in the CNG channels in *Drosophila* and *Caenorhabditis* (table 1). The high degree of evolutionary conservation presumably reflects the functional importance of the mutated amino acid positions. If the overall conservation of these sequences is taken into account, the difference in the distribution of mutations between evolutionarily conserved amino acid positions and non-conserved positions is highly significant ($P < .0001$).

Recurrent CNGA3 *Mutations: Frequency, Geographic Distribution, and Haplotypes*

Including the patients reported previously (Kohl et al. 1998), we identified a total of 110 of the 116 expected mutant alleles among our 58 independent patients with *CNGA3* mutations. Several mutations were found recurrently in different patients (table 1). The most prevalent mutations were R283W (19 mutant chromosomes), F547L (12 mutant chromosomes), R277C (9 mutant chromosomes), and R436W (6 mutant chromosomes). Together, these four mutations account for 46 of the 110 identified *ACHM2* chromosomes (41.8%). Whereas the high prevalence of the R283W mutation is due, in part, to homozygosity for this mutation (seven patients), the F547L, R277C, and R436W mutations were mostly observed in patients with compound-heterozygous mutations. The geographic distribution of these most-frequent recurrent mutations is quite different: although >40% (24/58) of patients with *CNGA3* mutations were of German origin, only 2 of the 12 patients with the R283W mutation were from Germany and the remainder were from Norway, Sweden, Denmark, and northern Italy. In contrast, all but one patient with the R436W mutation were of German origin. The most widespread distribution was observed for the F547L mutation, which was found in German, Dutch, Italian, Turkish, and Pakistani families.

To investigate the history of recurrent mutations, we reconstructed mutation-linked haplotypes, including three closely linked simple tandem repeat (STR) markers (*CNGA3-STR, D2S2311,* and *D2S2187*) and four intragenic single-nucleotide polymorphisms (SNPs) covering, altogether, a physical distance of ~170 kb around the *CNGA3* gene (fig. 1*a*).

We found evidence that, in some instances, recurrent mutations are of common origin, whereas, in others, they probably originate from independent mutation events. R410W- and R563H-linked haplotypes that differ from each other at several marker loci provide support for the latter interpretation. In both cases, those patients were of different geographic origin (Turkey vs. Germany and Turkey vs. Denmark; see fig. 3). Similarly, for the group of more frequent mutations, we propose multiple origins for the geographically most widespread F547L mutation and also for the geographically more restricted R436W chromosomes, albeit the degree of haplotype diversity differs between these two mutations. Among the nine reconstructed F547L chromosomes, three different haplotypes can be discerned: F547L-A: 288-T-A-G-C-158-158; F547L-B: 290-T-G-T-T-158-158; and F547L-C: 290/292-T-A-T-T-158-158 (marker order according to figs. 1*a* and 3). Haplotype F547L-C includes chromosomes with either the 290-bp or the 292-bp allele at marker *CNGA3-STR*. On the basis of the conservation of the SNP allele sequence, which occurs at a relative frequency of >.2 on control chromosomes ($n = 37$), this difference at *CNGA-STR* probably results from a recombination or a mutation at the STR locus. Since the observed 158-bp alleles at *D2S2311* and *D2S2187* represent the predominant marker alleles (relative frequencies .42 and .57, respectively, in control chromosomes), the presence of the same allele sequence (158-158) for these markers in all F547L haplotypes does not support a common origin. Interestingly, a common haplotype, F547L-A, was found on two F547L chromosomes present in Turkish patients as well as on another F547L chromosome from an Italian patient, consistent with a genetic exchange along the Mediterranean coast. Even more surprising, we found a common haplotype, F547L-C, shared by a German patient and a F547L homozygous patient originating from Pakistan.

Haplotype reconstruction allowed no convincing conclusions about the origin of the P163L and R277C mutations. In both groups, there are deviant haplotypes that differ from their counterparts only at one flank with respect to the mutation site (fig. 3). We cannot rule out an independent origin of these chromosomes; however, recombination events or mutations at marker loci might also have led to the deviation from the original haplotype. Since the majority of R277C mutant chromosomes share a common haplotype, 292-T-A-G-C-158-158, it is reasonable to propose that a founder effect at least contributes to the elevated frequency of this mutation.

In contrast, there is clear evidence for a monophyletic origin of the I312del mutation, as well as the R427C mutation. A complete correspondence of haplotypes was observed for the two I312del chromosomes reconstructed

Family	Origin	Mutation	*CNGA3* -*STR*	72 T→C	102-16 A→G	215+46 T→G	215+151 T→C	*D2S2311*	*D2S2187*
CHRO14	D	P163L	290	T	G	T	C	154	158
CHRO61	D	P163L	290	T	G	T	C	158	158
CHRO32	D	R277C	292	T	A	G	C	158	158
CHRO34	D	R277C	292	T	A	G	C	158	158
CHRO118	D	R277C	290/292	T	A	G	C	158	158
ZD95	D	R277C	290/292	T	A	G	C	154/158	158
CHRO65	D	R277C	290/292	T	A	T/G	T/C	158	158
CHRO159	NL	R277C	290/292	T	A	T/G	T/C	154/158	158
CHRO47	S	R277C	290	T	A	G	C	158	158
CHRO254	US	R277C	290	T	A	T	C	158	158
CHRO185	GR	R277C	290	C	G	T	C	158	158
CHRO18	N	R283W	292	T	A	T	C	158	160
CHRO48	S	R283W	292	T	A	T	C	158	160
CHRO50	S	R283W	292	T	A	T	C	158	160
CHRO127	DK	R283W	292	T	A	T	C	158	160
CHRO115	I	R283W	292	T	A	T	C	158	160
CHRO209	I	R283W	292	T	A	T	C	158	160
CHRO214	I	R283W(A)	292	T	A	T	C	158	160
CHRO124	D	R283W	292	T	A	T	T/C	158	160
ZD95	D	R283W	290/292	T	A	T	C	154/158	160
CHRO74	DK	R283W	290/292	T	A	T	C	158/160	160
CHRO214	I	R283W(B)	292	T	A	T	C	158	162
CHRO243	I	R283W	290	T	G	T	C	158	160
CHRO66	I	I312del	290	T	A	T	T	158	158
CHRO13	HT	I312del	290	T	A	T	T	158	158
CHRO15	D	R410W	290	T	G	T	C	154	158
CHRO101	TK	R410W	290	T	A	T	C	138	158
CHRO38	US	R427C	290	T	A	T	T	158	158
ZD128	D	R427C	290	T	A	T	T/C	158	158/162
CHRO65	D	R427C	290/292	T	A	T/G	T/C	158	158
CHRO61	D	R436W	290	T	G	T	C	154	158
CHRO202l	D	R436W	290	T	G	T	T/C	154	158
CHRO16	D	R436W	290	T	G/A	T	C	154/158	158
CHRO185	GR	R436W	292	T	A	T	T	154	158
ZD128	D	R436W	290	T	A	T	T/C	158	158/162
CHRO105	TK	F547L	288	T	A	G	C	158	158
ZD53	TK	F547L	288	T	A	G	C	158	158
CHRO235	I	F547L	288	T	A	G	C	154/158	158
CHRO32	D	F547L	290	T	G	T	T	158	158
CHRO202	D	F547L	290	T	G	T	T/C	158	158
CHRO113	PK	F547L	290	T	A	T	T	158	158
CHRO11	D	F547L	290	T	A	T	T	158	156/158
CHRO178	D	F547L	290/294	T/C	A	T	T/C	156/158	158
CHRO180	D	F547L	292	T	A	T	T	158	158
ZD53	TK	R563H	288	T	G	T	T	154	142
CHRO74	DK	R563H	290/292	T	A	T	C	158/160	160

Figure 3 Haplotypes of *CNGA3* mutant chromosomes. The origins of patients are given in the second column: D = Germany; DK = Denmark; GR = Greece; HT = Haiti; I = Italy; N = Norway; NL = The Netherlands; PK = Pakistan; S = Sweden; TK = Turkey; and US = United States. Similar haplotypes for a given mutation (which probably reflect a common origin) are boxed, and deviations within a group of similar haplotypes are represented by blank haplotype segments. The dark-shaded segment for CHRO180 represent a second-order haplotype deviation. The vertical line marked by an arrowhead represents the relative position of the mutations, between SNP 215+151T→C and *D2S2311*. Alleles of STR markers are given as fragment sizes.

in families CHRO13 and CHRO66 and can be also assumed for the R427C chromosomes, for which the phase at some markers could not be resolved experimentally.

Finally, we suggest a common origin of the R283W mutation, the most prevalent mutation in *CNGA3*. Haplotypes of 17 R283W chromosomes were reconstructed from 11 independent patients. Although parental consanguinity could not be established for the six patients

with homozygous R283W mutations, all but one were also homozygous for all tested markers and thus were considered as bearing a single haplotype identical-by-descent (IBD). In contrast, the two R283W chromosomes segregating in family CHRO214 differ at marker *D2S2187*. Therefore, we formally considered both R283W chromosomes segregating in this family as independent haplotypes. The final sample of R283W haplotypes used for comparison thus comprises five chromosomes representing the R283W homozygotes considered as IBD, the two R283W chromosomes segregating in family CHRO214, and another five R283W chromosomes from compound-heterozygous patients (fig. 3). Among this sample a common haplotype, 292-T-A-T-C-158-160, was seen on seven fully resolved R283W chromosomes and can be traced in three further R283W chromosomes with incompletely resolved allele assignment (CHRO74, CHRO124, and ZD95). Significantly, all these chromosomes share the 160-bp allele at marker *D2S2187,* which is uncommon in controls (relative frequency .16). The presence of this particular 160-bp allele on the R283W chromosome in family ACH09-1 suggests that its deviation from the common haplotype at marker *CNGA3-STR* and SNP 102-16A→G results from an intragenic recombination proximal to the mutation. A second deviant R283W chromosome was reconstructed in family CHRO214. Also, in this case, there are several reasons that favor a differentiation from the common haplotype rather than an independent origin of the R283W mutation. These include (*a*) the presence of a 162-bp allele at the most distal marker *D2S2187* being the only difference from the common R283W haplotype, (*b*) the fact that the conserved haplotype segment (*CNGA3-STR* through *D2S2311*) is rare in controls (relative frequency .03), and (*c*) the presence of a second R283W chromosome segregating in this family, which is unlikely to be encountered by chance.

In conclusion, these results strongly support the interpretation that all observed R283W chromosomes share a common origin. Given the unusual geographic distribution of the R283W mutation, we argue that, from a common ancestor, two separate founding populations have evolved that account for the elevated frequency of the R283W mutation in northern Europe and northern Italy.

Phenotypes of Patients with CNGA3 *Mutations*

Screening of a broad spectrum of cone photoreceptor disorders in the present study demonstrates that *CNGA3* mutations are not necessarily correlated with a phenotype of complete achromatopsia, as described previously, but can also be present in patients with other cone disorders. Clinical data were available for 67 patients with *CNGA3* mutations (table 2). Thirty-three patients from 26 families had a diagnosis of complete achromatopsia. Their visual acuities ranged from 0.05 to 0.16, except that one patient had a visual acuity of 0.2 in one eye. All patients lacked cone ERG responses under standard clinical setup and had no color vision. Photophobia was present in all patients and nystagmus in ~90% of the patients. Some of those without nystagmus at the time of examination had a history of a transient period of nystagmus during childhood. Refractive errors were quite variable, ranging from −6.0 to 13.0, but the majority of patients were hyperopic (mean spherical equivalent +1.72). There was no evidence for any disease progression after early childhood.

CNGA3 mutations were also found in 18 families comprising 20 patients with diagnoses of incomplete achromatopsia. The considerable variability in the clinical presentation among these patients probably reflects the extent of disturbance of the cone photoreceptor system. Whereas, in some patients, residual cone function could be detected only by psychophysical color vision testing, others showed sizeable cone ERGs and only slightly impaired color vision (e.g., siblings CHRO21/N and CHRO21/A). Visual acuities ranged from 0.06 to 0.6 and were, on average, better than those of complete achromats. Color-vision disturbances were rather nonuniform. Interestingly, some patients could perform color matches only for certain regions of the visual spectrum (e.g., residual blue-yellow discrimination). Not all incomplete achromats complained about photophobia. Those with the best preserved cone function had no or only moderate problems with daylight conditions. As in the group of complete achromats, hyperopia is the predominant refractive error in patients with incomplete achromatopsia (mean spherical equivalent +0.541).

The available clinical data for 11 patients did not suffice to categorize them reliably as complete or incomplete achromats. These cases are therefore presented as nonclassified cases in table 2.

Finally, three patients had a diagnosis of cone dystrophy. Current cone photoreceptor function parameters were similar to those observed in patients with achromatopsia, but there was evidence for a progression, either in follow-up examinations (ZD53/A) or subjectively reported by the patient (ZD82/H) and/or due to the presence of funduscopic abnormalities (ZD95/K and ZD82/H). In addition, two of these patients (ZD53/A and ZD95/K) showed reduced rod function in ERGs.

In most instances, affected siblings or patients with the same *CNGA3* genotype showed a similar clinical phenotype. A notable exception were the patients homozygous for the R283W mutation. Some of them were complete achromats with no detectable cone function, whereas others had residual cone ERG responses and/or color vision, justifying the diagnosis of incomplete achromatopsia (table 2; CHRO214/P and CHRO252/C).

Phenotype-genotype correlation in autosomal recessive

Table 2

Clinical Presentation of Patients with *CNGA3* Mutations

Patient[a,b]	Origin[c]	Age at Examination/Sex	Allele A[d]	Allele B[d]	Visual Acuity	Refraction[e]	Cone ERG	Color Vision	Photophobia	Nystagmus
Complete achromatopsia:										
CHRO135/H	NL	33/M	D162V	D260N	.16/.16	−.5/−1.0	No response	None	Yes	No
CHRO14/B^{+}	D	54/F	P163L*	P163L*	.1/.1	+.5/−.5	No response	None	Yes	Yes
CHRO61/198	D	21/M	P163L*	R436W*	.05/.05	+1.8/−2.75	No response	None	Yes	No
CHRO178/M	D	38/F	N182Y	F547L	.12/.12	−1.5/−2.25	No response	None	Yes	Yes
CHRO47/C	S	43/F	L186F*	R277C*	.15/.15	−1.75/−1.25	No response	None	Yes	Yes
CHRO118/399	D	20/M	C191Y*	R277C*	.2/.08	+1.5/+.8	No response	None	Yes	Yes
CHRO71/S	D	21/F	G267D*	Q655X*	.1/.08	−5.0/−6.0	No response	None	Yes	Yes
CHRO32/M	D	9/M	R277C*	F547L*	.1/.1	+6.0/+6.0	No response	None	Yes	Yes
CHRO159/T	NL	15/M	R277C	Y573C	.1/.1	+1.5/+1.0	No response	None	Yes	Yes
CHRO104/22	TK	6/M	R277H*	R277H*	.1/.1	+7.0/+7.0	No response	None	Yes	Yes
CHRO104/24	TK	15/F	R277H*	R277H*	.05/.05	+13.0/+13.0	No response	None	Yes	Yes
CHRO18/G^{+}	N	48/M	R283W	R283W	.1/.1	Hyperopic	No response	None	Yes	Yes
CHRO18/B^{+}	N	50/F	R283W	R283W	.1/.1	Hyperopic	No response	None	Yes	Yes
CHRO18/K^{+}	N	51/M	R283W	R283W	.1/.1	+8.0/+7.7	No response	None	Yes	Yes
CHRO127/L	DK	62/F	R283W	R283W	.05/.05	+1.25/+1.5	No response	None	Yes	Yes
CHRO124/C	D	10/F	R283W*	P372S*	.1/.1	+1.7/+1.7	No response	None	Yes	Yes
CHRO124/T	D	11/M	R283W*	P372S*	.1/.1	−2.2/−3.2	No response	None	Yes	Yes
CHRO48/EL	S	49/F	R283W*	F380S*	.1/.1	−2.0/−2.0	No response	None	Yes	Yes
CHRO66/G	I	10/M	I312del*	I312del*	.1/.1	−1.0/−1.5	No response	None	Yes	Yes
CHRO13/A	HT	9/F	I312del*	D485V*	.1/.1	−2.0/−3.0	No response	None	Yes	Yes
CHRO13/L	HT	12/F	I312del*	D485V*	.1/.05	+.5/+.5	No response	None	Yes	Yes
CHRO7/P	D	14/F	M406T	?	.1/.1	+3.75/+4.5	No response	None	Yes	Yes
CHRO15/M^{+}	D	47/F	R410W*	V529M*	.1/.1	+3.0/+5.25	No response	None	Yes	Yes
CHRO202/J	D	32/M	R436W*	F547L*	.1/.1	−3.25/−3.25	No response	None	Yes	Yes
CHRO103/Km	TK	7/M	W440X*	G516E*	.15/.15	+3.5/+3.0	No response	None	Yes	Yes
CHRO103/Kz	TK	7/F	W440X*	G516E*	.1/.15	+7.0/+7.0	No response	None	Yes	Yes
CHRO103/S	TK	14/M	W440X*	G516E*	.15/.15	+6.0/+5.0	No response	None	Yes	Transient
CHRO248/C	D	28/M	C510S	C510S	.1/.1	+4.5/+4.5	No response	None	Yes	No
CHRO258/S	I	9/F	G513E*	R569H*	.05/.05	−.75/−1.75	No response	None	Yes	Yes
CHRO235/1-1	I	12/M	F547L*	E194K*	.16/.12	+.75/+.25	No response	None	Yes	Yes
CHRO105/S	TK	8/M	F547L*	F547L*	.1/.1	+2.0/+1.75	No response	None	Yes	Yes
CHRO113/J	PK	27/M	F547L	F547L	.16/.1	Myopic	No response	None	Yes	No
CHRO180/T	D	13/M	F547L	?	.1/.1	+5.5/+6.0	No response	None	Yes	Yes
Incomplete achromatopsia:										
CHRO179/U	D	23/M	Y181C	Y181C	.2/.125	+2.0/+3.25	Reduced	Abnormal	Yes	Yes
CHRO241/7-1	I	13/M	C191Y*	C191Y*	.1/.1	+.75/+.75	Residual	Residual red	Yes	Yes

CHRO119/M	I	3/M	R223W*	S341P*	~.2/~.2	+.375/+.375	Residual	Abnormal	Moderate	Yes
CHRO21/A	D	13/F	T224R*	T369S*	.5/.3	+3.5/+3.75	Reduced	Slightly abnormal	Moderate	Yes
CHRO21/N	D	18/F	T224R*	T369S*	.6/.4	−5.5/−5.0	Reduced	Slightly abnormal	Moderate	Yes
CHRO65/A	D	18/F	R277C	R427C	.06/.05	+.75/−.25	Residual	Severely defective	Yes	Yes
CHRO254/A	US	7/M	R277C*	G557R*	.2/.12	+.75/+.75	No response	Residual blue	Yes	Yes
CHRO214/P	I	3/F	R283W*	R283W*	.1/.1	+3.5/+3.5	Strongly reduced	ND	Yes	Yes
CHRO252/C	I	4/M	R283W*	R283W*	.1/.1	+1.75/+1.75	Residual	None	Yes	Yes
CHRO74/B	DK	12/M	R283W	R563H	.15/.1	+3.75/+4.25	ND	Residual red and yellow	Yes	Yes
CHRO243/9-1	I	17/M	R283W*	T565M*	.1/.06	0/0	Response	Residual blue	Yes	Yes
CHRO11/L[+]	D	34/F	T291R*	F547L*	.1/.1	+6.0/+5.5	Reduced	Abnormal	Yes	Yes
CHRO11/W[+]	D	36/M	T291R*	F547L*	.2/.2	+3.0/+3.0	Reduced	Abnormal	Yes	No
ZD128/M	D	34/M	R427C	R436W	.125/.125	−12.0/−10.0	~80% reduced	Abnormal	Yes	Yes
CHRO38/M	US	40/F	R427C*	V451fs*	.2/.2	−2.0/0	No response	Abnormal	Yes	Yes
CHRO223/J	D	63/M	R436W	R563H	.1/.1	−.75/−.5	Strongly reduced	Abnormal	Yes	Mild
CHRO16/G	D	56/M	R436W	?	.1/.1	+5.6/+6.3	Residual	Severely defective	Yes	No
CHRO171/M	NL	16/M	I522T	F547L	.16/.16	−7.25/−9.75	ND	Abnormal	Yes	Yes
CHRO79/O	DK	56/M	G525D*	T565M*	.2/.16	+.25/0	Residual	Slightly abnormal	No	Yes
CHRO208/K	D	17/F	E593K	?	.1/.1	+4.0/+4.25	No response	Abnormal	Yes	Yes
Cone dystrophy:										
ZD95/K[f]	D	15/F	R277C*	R283W*	.05/.05	−6.5/−6.0	Absent	Defective	Yes	Yes
ZD82/H[g]	TK	23/F	N471S	?	.1/.1	−1.25/−1.0	Reduced	Abnormal	Yes	No
ZD53/A[h]	TK	32/F	R563H*	F547L*	<.05/<.05	+3.5/+2.5	Absent	Severely defective	Yes	Yes
Nonclassified:[i]										
CHRO220/217	B	ND/M	G49fs*	W316X*	No data available					
CHRO92/S	D	2/M	R223W*	R223W*	ND	+5.0/+5.75	ND	ND	Yes	Yes
CHRO185/M	GR	2/F	R277C*	R436W*	ND	+1.5/+1.5	ND	ND	Yes	Yes
CHRO34/831	D	59/F	R277C*	Q537X*	.2/.2	+3.8/+2.8	No response	None	Yes	No
CHRO6/S[+]	US	2/F	R283Q*	G557R*	No data available					
CHRO155/M	NL	25/M	R283Q	?	.16/.16	+3.0/+3.5	No response	ND	Yes	No
CHRO50/A	S	3/M	R283W*	R283W*	ND	ND	No response	ND	Yes	Yes
CHRO209/B	I	14/M	R283W*	R283W*	.2/.2	+3.5/+3.5	No response	Abnormal	Yes	Yes
CHRO115/H	I	25/M	R283W*	R283W*	.1/.1	−1.25/−2.0	ND	None	Yes	Yes
CHRO121/N	TU	5/F	P372S*	P372S*	.15/.15	−.75/+1.5	ND	None	Yes	Yes
CHRO101/A	TK	6/F	R410W*	R410W*	.1/.1	−3.5/−3.5	No response	ND	Yes	Yes

[a] Patients with identical identifiers to the left of the slash belong to the same family.

[b] A plus sign (+) denotes patients from families reported by Kohl et al. (1998).

[c] B = Belgium, D = Germany, DK = Denmark, GR = Greece, HT = Haiti, I = Italy, N = Norway, NL = The Netherlands, PK = Pakistan, S = Sweden, TK = Turkey, TU = Tunisia, and US = United States.

[d] An asterisk (*) denotes patients in whom homozygosity or allelism of heterozygous mutations could be established by segregation analysis. A question mark (?) denotes patients with single heterozygous mutations.

[e] Refractive errors are given in spherical equivalents.

[f] The patient shows a bull's eye maculopathy and a reduced scotopic ERG.

[g] This patient's age at onset was 10 years with rapid visual loss macular changes.

[h] This patient showed a reduction in visual acuity in follow-up examination, a progressive visual field loss, and a reduced scotopic ERG.

[i] Individuals not classified because of inconclusive clinical data.

conditions is principally complicated by the uncertainty, in compound heterozygotes, about which of the two mutant alleles retains the crucial functional activity, about whether both mutant alleles act synergistically and about whether they can complement each other. Despite these inherent limitations, it is noteworthy that the R427C, R563H, and T565M mutations have been exclusively found in patients with incomplete achromatopsia or cone dystrophy and thus represent the best candidates for mutations that do not completely abolish cone photoreceptor function. Interestingly, we found that two of the patients with the least severe visual complaints (CHRO21 and CHRO119) were both compound heterozygotes for mutations in the cytoplasmic linker between transmembrane domains S2 and S3 and in the channels' pore regions (T224R/T369S and R223W/S341P, respectively).

It has been shown that the murine and bovine orthologues of the human *CNGA3* gene are also expressed in nonretinal tissues, notably kidney, testis, and the pineal gland (Biel et al. 1994). However, none of the patients with *CNGA3* mutations had a positive medical history for systemic disease and evaluation of self-assessment patient questionnaires (13 respondents) revealed no evidence that mutations in the *CNGA3* gene were associated with other, nonvisual illnesses or complaints.

Discussion

We have recently shown that mutations in the *CNGA3* gene cause complete achromatopsia (Kohl et al. 1998). One of the major findings of the present study is that *CNGA3* mutations do not only lead to complete achromatopsia but can also cause incomplete achromatopsia with residual cone function. The phenotypic presentation of such incomplete achromats is highly variable, ranging from cases with barely detectable remnants of color vision to those with well-preserved visual acuity and only slightly abnormal color vision. Some of the incomplete achromats with *CNGA3* mutations showed residual color-sensitivity only for parts of the visual spectrum rather than a uniform defect. This peculiar variability in color sensitivity has already been noticed in early clinical descriptions of incomplete achromats (Jäger 1953; Goodman et al. 1963). We also found that disease expression can vary among siblings or patients with the same *CNGA3* genotype. For example, on detailed electrophysiological and psychophysical investigations, apparent differences in the extent of cone dysfunction were found between the affected siblings in family CHRO21, who had the least severe visual complaints of all patients with *CNGA3* mutations (H. Jägle and L. T. Sharpe, unpublished data). The phenotypic variability in these patients with rather well-preserved cone function may result from differences in lens density and macular pigment (Stockman and Sharpe 1999), as well as from differences in the S- to M- to L-cone ratio and distribution (Hagstrom et al. 1998; Roorda and Williams 1999) or the presence of simultaneous alterations in the pigment genes. Furthermore, some patients homozygous for the R283W mutations present as complete achromats, whereas others had some residual cone function, although at a low level. It is noteworthy that the latter were young children (3 and 4 years of age at examination), in contrast to the four R283W homozygotes diagnosed as complete achromats, all of whom were $\geqslant$48 years old. This may indicate that, in R283W homozygotes, there is a loss of the residual cone function during the patient's lifetime, resulting in discrepant clinical presentation depending on the patients' age at examination. However, a progressive loss of cone function as a general mechanism in achromatopsia is unlikely, since the mean ages (at examination) of complete and incomplete achromats were nearly identical (24.39 years vs. 24.15 years). Thus, we have to consider that other factors—like the precise sequence and expression of the channel β-subunit or the total number of defective cones that are actually formed in retinal development—determine the actual clinical phenotype in patients with the same genotype. Such anticipated distortions in the development of cone photoreceptors and the cone mosaic are documented from the homologous knockout-mouse model (Biel et al. 1999) and the sparse histological studies of retinae from achromats (Larsen 1921; Harrison et al. 1960; Falls et al. 1965; Glickstein and Heath 1975).

The definite categorization of patients as complete or incomplete achromats can be difficult in those cases with very low cone function and mainly relies on the sensitivity and reliability of noninvasive clinical and psychophysical testing. Because of these diagnostic limitations and the fact that complete and incomplete achromatopsia are caused by mutations in the same gene, both disorders should rather be considered as part of a continuous clinical spectrum of cone photoreceptor dysfunction. Nevertheless, the availability of genotype data now reinforces the demand for the development of improved noninvasive clinical tests and their standardization, to resolve subtle phenotypic differences.

Some patients with *CNGA3* mutations had a diagnosis of cone dystrophy. These patients tended to be the ones with the most-severe clinical symptoms among the group of cone dystrophy patients analyzed in this study (for a review about the clinical presentation, see the report by Kellner [1996]). However, since the evidence for the presence of a progressive retinal dystrophy is still limited in these cases, further follow-up examinations and the identification of additional affected individuals will be necessary to confirm these findings.

Heterozygotes for *CNGA3* mutations do not complain of any visual problems and their cone photoreceptor function is normal (H. Jägle and L. T. Sharpe, unpublished data), indicating that *CNGA3* mutations

behave in a strictly recessive manner. In patients with residual cone function, either one or both mutant alleles gives rise to some functional CNG channel activity, or the two mutant channels complement each other for functional activity. Although the assignment of functional activity is hampered by a limited phenotype-genotype correlation, some alleles with mutations in the pore region (S341P and T369S) or in the cGMP-binding domain (R563H and T565M) are prime candidates for encoding such cone CNG channels with some retained functional activity. Further experimental evidence for this assumption and the elucidation of the molecular pathology might be obtained from the analysis of in vitro–expressed mutant CNG channels.

In the present study, we were able to identify *CNGA3* mutations in 53 index patients. Among them, 16 had apparently homozygous mutations and another 31 carried two heterozygous mutations. True homozygosity in the former patients and compound heterozygosity in the latter could be established in all cases in which additional samples from family members were available for segregation analysis (12/16 and 23/31, respectively). For the remainder, we cannot formally exclude other scenarios (e.g., heterozygous deletions or presence of mutations in *cis*). Merely single heterozygous mutations were found in six additional patients. The simplest explanation for these cases is that we failed to detect the second mutation—which may be located in as yet unidentified regulatory domains of the *CNGA3* gene—or that some disease alleles constitute larger deletions that have not been ruled out in all cases. A dominant effect of these mutations can be excluded in most cases. Three of these patients (CHRO180/T, CHRO16/G, and CHRO155/M; see table 2) carry known mutations that were also found in patients with compound-heterozygous mutations. For two further patients (CHRO7/P and CHRO208/K) there were also unaffected family members who possess the corresponding mutant allele.

Only ~25% of patients with achromatopsia carry mutations in the *CNGA3* gene. Recently, a second locus for achromatopsia (*ACHM3*) has been localized on chromosome 8q21 (Milunsky et al. 1999; Winick et al. 1999), and, subsequently, we and others have shown that mutations in the *CNGB3* gene encoding the β-subunit of the cone cGMP-gated channel are responsible for achromatopsia in patients who show linkage to this locus (Kohl et al. 2000; Sundin et al. 2000). Preliminary data indicate that mutations in the *CNGB3* gene are more prevalent in achromats than are those in the *CNGA3* gene (B. Wissinger and S. Kohl, unpublished data).

Contrary to the expectations for a recessively inherited disorder, the vast majority of mutations in the *CNGA3* gene represent missense mutations. This indicates that there is little tolerance for substitutions with respect to functional maintenance of the channel polypeptide. This notion is supported by the high degree of evolutionary conservation not only for *CNGA3* orthologues in different species but also for functional paralogues in the vertebrate rod photoreceptor and olfactory epithelium and sensory CNG channels in *Drosophila* and *Caenorhabditis*.

Although the majority of mutations are located in structurally and functionally important parts of the CNGA3 polypeptide (i.e., the transmembrane helices, the pore, and the cGMP-binding domain), we observed a considerable number of missense mutations in less-well-characterized parts of the protein—in particular, the linking segments between S1 and S2 and between S6 and the cGMP-binding domain. The functional contribution of these parts of the protein and the kind of defect resulting from mutations therein remains to be established by further functional analysis and biophysical characterization of the CNGA3 channel.

Most *CNGA3* mutations were observed only once, either in the heterozygous state or in the homozygous state in cases with known or suspected parental consanguinity. However, a few mutations—in particular, R283W, F547L, R277C, and R436W—were found recurrently in several independent patients and accounted for a substantial portion of all mutant alleles. Haplotype analysis suggests that the F547L mutation has multiple origins, whereas the R427C chromosomes, as well as the R283W chromosomes, are genetically related and probably originate from a common ancestral mutation. Interestingly, we found the R283W mutation to be most prevalent among patients from Scandinavia and northern Italy. Since both regional groups share a common haplotype, there must have been a genetic interchange in the past between these distant regions, followed by a regional spreading of this particular disease allele.

We have presented a first comprehensive screening analysis of *CNGA3* in patients with cone photoreceptor disorders. Although this study now provides the first data set on the prevalence of *CNGA3* mutations and the associated spectrum of phenotypes, additional functional studies analyzing their pathophysiological effects on the cone CNG channel, the phototransduction cascade, and retinal development will be necessary to decipher the molecular pathology of cone photoreceptor disorders caused by *CNGA3* mutations.

Acknowledgments

We would like to thank all patients and their families, for participating in this study; Nurten Akarsu, Alessandra Maugheri, Elaine de Castro, David Hanna, and Markus Preising, for sample collection, sample preparation, and logistics; and Sigrun Klessinger and Hermann Krastel, for initial referral of patients. We also thank Francis Futterman and Elisabetta Lu-

chetta, for promoting information about and research on achromatopsia and for logistic help, and Dimitri Tränkner, Reinhard Seifert, U. Benjamin Kaupp, and Klaus Benndorff, for helpful discussions on the physiology and biophysics of CNG channels. We kindly acknowledge the provision of filters of the Lawrence Livermore National Laboratory chromosome 2 PAC library and pools of the Roswell Park Cancer Institute PAC libraries through the Human Genome Mapping Project Resource Center, Hinxton, United Kingdom. This work was supported by a grant of the Federal Ministry of Education, Science, Research, and Technology (Fö. 01KS9602) and the Interdisciplinary Center for Clinical Research, Tübingen, (to L.T.S.) and grants of the Deutsche Forschungsmeinschaft (SFB430/A5) and the *fortüne* research program (grant 583) of the Medical Faculty of the Tübingen University (to B.W.).

Electronic-Database Information

Accession numbers and URLs for data in this article are as follows:

GenBank, http://www.ncbi.nlm.nih.gov/ (for the CNG channel α-subunits of human cone photoreceptors [accession number AF065314], of mouse cone photoreceptors [accession number AJ243933], of chicken cone photoreceptors [accession number X89598], of human rod photoreceptors [accession number S42457], and of the bovine olfactory epithelium [accession number X55010], the *Drosophila melanogaster* CNG channel [accession number X89601], the *Caenorhabditis elegans tax4* CNG channel [accession number D89601], and the CGNA3-covering BAC clones RP11-127K18 [accession number AC010134] and RP11-127K18 [accession number AC010134])

Online Mendelian Inheritance in Man (OMIM), http://www.ncbi.nlm.nih.gov/Omim/ (for ACHM2 [MIM 216900], ACHM3 [MIM 262300], BCM [MIM 303700], CNGA3 [MIM 600053], and CNGB3 [MIM 605080])

References

Andreasson S, Tornqvist K (1991) Electroretinograms in patients with achromatopsia. Acta Ophthalmol 69:711–716

Arbour NC, Zlotogora J, Knowlton RG, Merin S, Rosenmann A, Kanis AB, Rokhlina T, Stone EM, Sheffield VC (1997) Homozygosity mapping of achromatopsia to chromosome 2 using DNA pooling. Hum Mol Genet 6:689–694

Ayyagari R, Kakuk LE, Coats CL, Bingham EL, Toda Y, Felius J, Sieving PA (1999) Bilateral macular atrophy in blue cone monochromacy (BCM) with loss of the locus control region (LCR) and part of the red pigment gene. Mol Vis 5:13

Biel M, Seeliger M, Pfeifer A, Kohler K, Gerstner A, Ludwig A, Jaissle G, Fauser S, Zrenner E, Hofmann F (1999) Selective loss of of cone function in mice lacking the cyclic nucleotide-gated channel CNG3. Proc Natl Acad Sci USA 96:7553–7557

Biel M, Zong X, Distler M, Bosse E, Klugbauer N, Murakami M, Flockerzi V, Hofmann F (1994) Another member of the cyclic nucleotide-gated channel family, expressed in testis, kidney, and heart. Proc Natl Acad Sci USA 91:3505–3509

Dryja TP, Finn JT, Peng YW, McGee TL, Berson EL, Yau KW (1995) Mutations in the gene encoding the α-subunit of the rod cGMP-gated channel in autosomal recessive retinitis pigmentosa. Proc Natl Acad Sci USA 92:10177–10181

Falls HF, Wolter JR, Alpern M (1965) Typical total monochromacy. Arch Ophthalmol 74:610–616

Francois J (1961) Heredity in ophthalmology. CV Mosby, St Louis

Gingrich JC, Boehrer D, Garnes JA, Johnson W, Wong B, Bergmann A, Eveleth GG, Longlois RG, Carrano AV (1996) Construction and characterization of human chromosome 2 specific cosmid, fosmid and PAC clone libraries. Genomics 32:65–74

Glickstein M, Heath GG (1975) Receptors in the monochromat eye. Vision Res 15:633–636

Goodman G, Ripps H, Siegel IM (1963) Cone dysfunction syndromes. Arch Ophthalmol 70:214–231

Hagstrom SA, Neitz J, Neitz M (1998) Variations in the cone population for red-green color vision examined by analysis of mRNA. Neuroreport 9:1963–1967

Hansen E (1979) Typical and atypical monochromacy studied by specific quantitative perimetry. Acta Ophthalmol 57: 211–224

Harrison H, Hoefnagel D, Hayward JN (1960) Congenital total colorblindness, a clinico-pathological report. Arch Ophthalmol 64:685–692

Ioannou PA, de Jong PJ (1996) Construction of bacterial artificial chromosome libraries using a modified P1 (PAC) system. In: Dracopoli NC, Haines JL, Korf BR, Moir DT, Morton CC, Seidman CE, Seidman JG, Smith DR (eds) Current protocols in human genetics. John Wiley & Sons, New York

Jäger W (1953) Typen der inkompletten Achromatopsie. Berl Dtsch Ophthalmol Ges 58:44–47

Jägle H, Kohl S, Apfelstedt-Sylla E, Wissinger B, Sharpe LT (2001) Manifestation of rod monochromacy. Col Res Appl 13:96–99

Kellner U (1996) Die progressiven Zapfendystrophien. Bücherei des Augenarztes Bd. 135, Enke Verlag, Stuttgart

Kohl S, Baumann B, Broghammer M, Jägle H, Sieving P, Kellner U, Spegal R, Anastasi M, Zrenner E, Sharpe LT, Wissinger B (2000) Mutations in the CNGB3 gene encoding the β-subunit of the cone photoreceptor cGMP-gated channel are responsible for achromatopsia (ACHM3) linked to chromosome 8q21. Hum Mol Genet 9:2107–2116

Kohl S, Marx T, Giddings I, Jägle H, Jacobson SG, Apfelstedt-Sylla E, Zrenner E, Sharpe LT, Wissinger B (1998) Total colourblindness is caused by mutations in the gene encoding the α-subunit of the cone photoreceptor cGMP-gated cation channel. Nat Genet 19:257–259

Larsen H (1921) Demonstration mikroskopischer Präparate von einem monochromatischen Auge. Klin Mbl Augenheilk 67:301–302

Milunsky A, Huang XL, Milunsky J, DeStefano A, Baldwin CT (1999) A locus for autosomal recessive achromatopsia on human chromosome 8q. Clin Genet 56:82–85

Müller F, Kaupp, UB (1998) Signaltransduktion in Sehzellen. Naturwissenschaften 85:49–61

Nathans J, Maumenee IH, Zrenner E, Sadowski B, Sharpe LT, Lewis RA, Hansen E, Rosenberg T, Schwartz M, Heckenlively JR, Traboulsi E, Klingaman R, Bech-Hansen NT, LaRoche GR, Pagon RA, Murphey WH, Weleber RG (1993)

Genetic heterogeneity among blue-cone monochromats. Am J Hum Genet 53:987–1000

Nathans J, Piantanida TP, Eddy RL, Shows TB, Hogness DS (1986) Molecular genetics of inherited variation in human color vision. Science 232:203–210

Neuhann T, Krastel H, Jaeger W (1978) Differential diagnosis of typical and atypical congenital achromatopsia: analysis of a progressive foveal dystrophy and a nonprogressive oligocone trichromasy (general cone dysfunction without achromatopsia), both of which at first had been diagnosed as achromatopsia. Albert Von Graefes Arch Klin Exp Ophthalmol 209:19–28

Roorda A, Williams DR (1999) The arrangement of the three cone classes in the living human eye. Nature 397:520–522

Sharpe LT, Nordby K (1990) Total colour blindness: an introduction. In: Hess RF, Sharpe LT, Nordby K (eds) Night vision: basic, clinical and applied aspects. Cambridge University Press, Cambridge, pp 253–289

Sharpe LT, Stockman A, Jägle H, Nathans J (1999) Opsin genes, cone photopigments and colorblindness. In: Gegenfurtner K, Sharpe LT (eds) Color vision: from genes to perception. Cambridge University Press, Cambridge, pp 3–52

Stockman A, Sharpe LT (1999) Cone spectral sensitivities and color matching. In: Gegenfurtner K, Sharpe LT (eds) Color vision: from genes to perception. Cambridge University Press, Cambridge, pp 53–87

Sundin OH, Yang JM, Li Y, Zhu D, Hurd JN, Mitchell TN, Silva ED, Hussels-Maumenee I (2000) Genetic basis of total colourblindness among the Pingelapese islanders. Nat Genet 25:289–293

Weitz CJ, Miyake Y, Shinzato K, Montag E, Zrenner, E, Went LN, Nathans N (1992) Human tritanopia associated with two amino acid substitutions in the blue sensitive opsin. Am J Hum Genet 50:498–507

Winick JD, Blundell ML, Galke BL, Salam AA, Leal SM, Karayiorgou M (1999) Homozygosity mapping of the achromatopsia locus in the Pingelapese. Am J Hum Genet 64: 1679–1685

Wissinger B, Jagle H, Kohl S, Broghammer M, Baumann B, Hanna DB, Hedels C, Apfelstedt-Sylla E, Randazzo G, Jacobson SG, Zrenner E, Sharpe LT (1998) Human rod monochromacy: linkage analysis and mapping of a cone photoreceptor expressed candidate gene on chromosome 2q11. Genomics 51:325–331

Wissinger B, Muller F, Weyand I, Schuffenhauer S, Thanos S, Kaupp UB, Zrenner E (1997) Cloning, chromosomal localization and functional expression of the gene encoding the alpha-subunit of the cGMP-gated channel in human cone photoreceptors. Eur J Neurosci 9:2512–2521

Zagotta WN, Siegelbaum SA (1996) Structure and function of cyclic nucleotide-gated channels. Annu Rev Neurosci 19:235–263

Zrenner E, Magnussen S, Lorenz B (1988) Blauzapfenmonochromasie: Diagnose, genetische Beratung, optische Hilfsmittel. Klin Mbl Augenheilk 193:510–517